

# Hidden-bottom molecular states from $\Sigma_b^{(*)}B^{(*)} - \Lambda_b B^{(*)}$ interaction

Jun-Tao Zhu, Shu-Yi Kong, Yi Liu, Jun He<sup>a</sup>

<sup>1</sup>Department of Physics and Institute of Theoretical Physics, Nanjing Normal University, Nanjing 210097, China

Received: date / Revised version: date

**Abstract** In this work, we study possible hidden-bottom molecular pentaquarks  $P_b$  from coupled-channel  $\Sigma_b^{(*)}B^{(*)} - \Lambda_b B^{(*)}$  interaction in the quasipotential Bethe-Salpeter equation approach. In isodoublet sector with  $I = 1/2$ , with the same reasonable parameters the interaction produces seven molecular states, a state near  $\Sigma_b B$  threshold with spin parity  $J^P = 1/2^-$ , a state near  $\Sigma_b^* B$  threshold with  $3/2^-$ , two states near  $\Sigma_b B^*$  threshold with  $1/2^-$  and  $3/2^-$ , and three states near  $\Sigma_b^* B^*$  threshold with  $1/2^-$ ,  $3/2^-$ , and  $5/2^-$ . The results suggest that three states near  $\Sigma_b^* B^*$  threshold and two states near  $\Sigma_b B^*$  threshold are very close, respectively, which may be difficult to distinguish in experiment without partial wave analysis. Compared with the hidden-charm pentaquark, the  $P_b$  states are relatively narrow with widths at an order of magnitude of 1 MeV or smaller. The importance of each channel considered is also discussed, and it is found that the  $\Lambda_b B^*$  channel provides important contribution for the widths of those states. In isoquartet sector with  $I = 3/2$ , cut-off should be considerably enlarged to achieve bound states from the interaction, which makes the existence of such states unreliable. The results in the current work are helpful for searching for hidden-bottom molecular pentaquarks in future experiments, such as the COMPASS, J-PARC, and the Electron Ion Collider in China (EicC).

## 1 INTRODUCTION

It is one of the most important topic in hadron physics community to search for the hadronic exotic states beyond the conventional quark model. Among the theoretical pictures in the market, molecular state is a competitive one to explain existing candidates of exotic states, such as the  $XYZ$  particles and  $P_c$  states [1]. A molecular state is analogous to a nucleus, especially the deuteron, that is, a loosely bound state

of two or more hadrons. It immediately leads to a conclusion that a molecular state is close to the threshold of constituent hadrons. In practice, the study of the molecular state also focuses on resonance structures near thresholds. Vice versa, if we can find more structures near thresholds, especially those with corresponding relationship, it will strongly support existence of molecular states. In the current work, we will provide predictions of hidden-charm pentaquarks  $P_b$ , which are partners of the hidden-charm  $P_c$  states.

The observation of hidden-charm pentaquarks at LHCb is a great breakthrough of the study of exotic states [2, 3]. It is also an important support on the molecular state picture. Three narrow resonance structures were reported at LHCb in an update measurement as  $P_c(4457)$  and  $P_c(4440)$  states near  $\Sigma_c \bar{D}^*$  threshold and a  $P_c(4312)$  state near  $\Sigma_c \bar{D}$  threshold [2]. Combined with  $P_c(4380)$  near  $\Sigma_c^* \bar{D}$  threshold suggested in the first observation [3], it exhibits a good pattern of the S-wave molecular states from interactions corresponding to the thresholds. Such observation confirms the prediction of existence of the hidden-charm pentaquark in some models [4–8].

A lot of theoretical interpretations of these structures emerged after the experimental observation. Due to the strong correlation between these structures and the thresholds, the molecular state is the most popular picture to explain the  $P_c$  states [9–17], though other interpretations can not be excluded [18–21]. In Ref. [22], authors even proposed existence of seven hidden-charm molecular states as a complete heavy-quark spin symmetry multiplet. In our previous works [23, 24], we systematically investigate coupled-channel  $\Sigma_c^{(*)} \bar{D}^{(*)} - \Lambda_c \bar{D}^{(*)}$  interaction. Three isodoublet states with  $I = 1/2$  are produced near  $\Sigma_c \bar{D}$  threshold with spin parity  $J^P = 1/2^-$  and  $\Sigma_c \bar{D}^*$  threshold with  $1/2^-$  and  $3/2^-$ . Their masses and widths fall well in the ranges of experimental values of the  $P_c(4312)$ ,  $P_c(4440)$  and  $P_c(4457)$  observed at LHCb. A state almost on the  $\Sigma_c^* \bar{D}^*$  thresh-

<sup>a</sup>Corresponding author: junhe@njnu.edu.cn

old with  $3/2^-$  is also produced and can be related to the  $P_c(4380)$ . Two another states near  $\Sigma_c^* \bar{D}^*$  threshold with  $1/2^-$  and  $3/2^-$  were also produced with the same parameters, but the result suggests that their effects on the experimental observable may be small. Besides, the decay pattern was also discussed, and the  $\Lambda \bar{D}^*$  channel is found dominant in the decays of these states.

Now that experimentally observed  $P_c$  states were well interpreted in the molecular state picture, we can predict hidden-bottom states above 11 GeV. Though there are a large amount of works about  $P_c$  states reported in the literature, the studies about the hidden-bottom pentaquark are still inadequate. There are a few incidental studies about  $P_b$  states in the works to interpret the  $P_c$  states in the molecular picture, such as within constituent quark model [17, 25], the chiral effective field theory [9, 26], and the Bethe-Salpeter equation [27]. The width and decay pattern of the  $P_b$  states were also discussed in Refs. [17, 27–30]. Due to very large mass of the hidden-bottom pentaquark, it is relatively difficult to search for the  $P_b$  state in experiment compared with the  $P_c$  state. In Ref. [31], pion and photon induced productions of hidden-bottom pentaquarks were studied, the calculation suggests that it is possible to search for these states at COMPASS, J-PARC and EicC. Hence, it is interesting to perform a systematical study about the hidden-charm pentaquarks based on experimental information and theoretical analysis about the  $P_c$  states.

In this work, we will investigate coupled-channel  $\Sigma_b^{(*)} B^{(*)} - \Lambda_b B^{(*)}$  interaction in the quasipotential Bethe-Salpeter equation (qBSE) approach to find possible hidden-bottom molecular states. The interaction was described in the one-boson-exchange model with the help of the effective Lagrangians within the heavy quark symmetry and chiral limit as in Refs. [23, 24], where the  $P_c$  states were interpreted. The masses and widths of molecular states are predicted by finding poles in complex energy plane. The decay channels of predicted states will be discussed also.

This article is organized as follows. After introduction, the details of theoretical frame of coupled-channel  $\Sigma_b^{(*)} B^{(*)} - \Lambda_b B^{(*)}$  interactions is presented in section 2. In Section 3, the single-channel results of the states with isospin  $I = 1/2$  and  $I = 3/2$  are given first. Then, coupled-channel results are presented, and the importance of the channels considered are discussed. Finally, summary and discussion will be given in section 4.

## 2 Theoretical frame

In the qBSE approach, we will use the one-boson-exchange interaction of two bottom hadrons as dynamical kernel. In the current work, we will adopt the Lagrangians with heavy quark limit and chiral symmetry, and the channels with hidden-charm mesons are ignored as in Ref. [23, 24] to keep

the consistence. The pseudoscalar  $\mathbb{P}$ , vector  $\mathbb{V}$  and scalar  $\sigma$  exchanges will be considered, and the effective Lagrangians depicting the couplings of light mesons and bottom mesons or bottom baryons are required and will be presented in the below.

First, we consider the couplings of light mesons to heavy-light bottom mesons  $\mathcal{P} = (B^0, B^+, B_s^+)$ . The Lagrangians were constructed in the literature as [32–35],

$$\begin{aligned}\mathcal{L}_{\mathcal{P}^* \mathcal{P} \mathbb{P}} &= i \frac{2g \sqrt{m_{\mathcal{P}} m_{\mathcal{P}^*}}}{f_{\pi}} (-\mathcal{P}_{a\lambda}^{*\dagger} \mathcal{P}_b + \mathcal{P}_a^{\dagger} \mathcal{P}_{b\lambda}^*) \partial^{\lambda} \mathbb{P}_{ab}, \\ \mathcal{L}_{\mathcal{P}^* \mathcal{P}^* \mathbb{P}} &= -\frac{g}{f_{\pi}} \epsilon_{\alpha\mu\nu\lambda} \mathcal{P}_a^{*\mu\dagger} \overleftrightarrow{\partial}^{\alpha} \mathcal{P}_b^{*\lambda} \partial^{\nu} \mathbb{P}_{ba}, \\ \mathcal{L}_{\mathcal{P}^* \mathcal{P} \mathbb{V}} &= \sqrt{2} \lambda g_V \epsilon_{\lambda\alpha\beta\mu} (-\mathcal{P}_a^{*\mu\dagger} \overleftrightarrow{\partial}^{\lambda} \mathcal{P}_b + \mathcal{P}_a^{\dagger} \overleftrightarrow{\partial}^{\lambda} \mathcal{P}_b^{*\mu}) (\partial^{\alpha} \mathbb{V}^{\beta})_{ab}, \\ \mathcal{L}_{\mathcal{P} \mathcal{P} \mathbb{V}} &= -i \frac{\beta g_V}{\sqrt{2}} \mathcal{P}_a^{\dagger} \overleftrightarrow{\partial}^{\mu} \mathcal{P}_b \mathbb{V}_{ab}^{\mu}, \\ \mathcal{L}_{\mathcal{P}^* \mathcal{P}^* \mathbb{V}} &= -i \frac{\beta g_V}{\sqrt{2}} \mathcal{P}_a^{*\dagger} \overleftrightarrow{\partial}^{\mu} \mathcal{P}_b^{*\nu} \mathbb{V}_{ab}^{\mu} - i2 \sqrt{2} \lambda g_V m_{\mathcal{P}^*} \mathcal{P}_a^{*\mu\dagger} \mathcal{P}_b^{*\nu} \mathbb{V}_{\mu\nu ab}, \\ \mathcal{L}_{\mathcal{P} \mathcal{P} \sigma} &= -2g_s m_{\mathcal{P}} \mathcal{P}_a^{\dagger} \mathcal{P}_a \sigma, \\ \mathcal{L}_{\mathcal{P}^* \mathcal{P}^* \sigma} &= 2g_s m_{\mathcal{P}^*} \mathcal{P}_a^{*\dagger} \mathcal{P}_a^* \sigma,\end{aligned}\quad (1)$$

where  $f_{\pi} = 132$  MeV,  $\mathbb{V}_{\mu\nu} = \partial_{\mu} \mathbb{V}_{\nu} - \partial_{\nu} \mathbb{V}_{\mu}$ , and the  $\nu$  is replaced by  $i \overleftrightarrow{\partial} / \sqrt{m_i m_f}$  with the  $m_{i,f}$  being mass of initial or final  $B^{(*)}$  meson. The  $\mathcal{P}$  and  $\mathcal{P}^*$  satisfy the normalization relations  $\langle 0 | \mathcal{P} | \bar{Q} q (0^-) \rangle = \sqrt{M_{\mathcal{P}}}$  and  $\langle 0 | \mathcal{P}_{\mu}^* | \bar{Q} q (1^-) \rangle = \epsilon_{\mu} \sqrt{M_{\mathcal{P}^*}}$ . The  $\mathbb{P}$  and  $\mathbb{V}$  are the pseudoscalar and vector matrices as

$$\mathbb{P} = \begin{pmatrix} \frac{\sqrt{3}\pi^0 + \eta}{\sqrt{6}} & \pi^+ & K^+ \\ \pi^- & -\frac{\sqrt{3}\pi^0 + \eta}{\sqrt{6}} & K^0 \\ K^- & \bar{K}^0 & -\frac{2\eta}{\sqrt{6}} \end{pmatrix}, \quad \mathbb{V} = \begin{pmatrix} \frac{\rho^0 + \omega}{\sqrt{2}} & \rho^+ & K^{*+} \\ \rho^- & -\frac{\rho^0 + \omega}{\sqrt{2}} & K^{*0} \\ K^{*-} & \bar{K}^{*0} & \phi \end{pmatrix}. \quad (2)$$

The explicit forms of the Lagrangians for the couplings of light mesons to bottom baryons can be written as [36],

$$\begin{aligned}\mathcal{L}_{BB\mathbb{P}} &= i \frac{3g_1}{2f_{\pi} \sqrt{m_{\bar{B}} m_B}} \epsilon^{\mu\nu\lambda\kappa} \partial^{\nu} \mathbb{P} \sum_{i=0,1} \bar{B}_{i\mu} \overleftrightarrow{\partial}_{\kappa} B_{j\lambda}, \\ \mathcal{L}_{BB\mathbb{V}} &= -\frac{\beta_S g_V}{\sqrt{2} m_{\bar{B}} m_B} \mathbb{V}^{\nu} \sum_{i=0,1} \bar{B}_i^{\mu} \overleftrightarrow{\partial}_{\nu} B_{j\mu} - \frac{\lambda_S g_V}{\sqrt{2}} \mathbb{V}_{\mu\nu} \sum_{i=0,1} \bar{B}_i^{\mu} B_j^{\nu}, \\ \mathcal{L}_{B_3 B_3 \mathbb{V}} &= -\frac{g_V \beta_B}{\sqrt{2} m_{\bar{B}_3} m_{B_3}} \mathbb{V}^{\mu} \bar{B}_3^{\nu} \overleftrightarrow{\partial}_{\mu} B_3, \\ \mathcal{L}_{BB_3 \mathbb{P}} &= -i \frac{g_4}{f_{\pi}} \sum_i \bar{B}_i^{\mu} \partial_{\mu} \mathbb{P} B_3 + \text{H.c.}, \\ \mathcal{L}_{BB_3 \mathbb{V}} &= \sqrt{\frac{2}{m_{\bar{B}} m_{B_3}}} g_V \lambda_I \epsilon^{\mu\nu\lambda\kappa} \partial_{\lambda} \mathbb{V}_{\kappa} \sum_i \bar{B}_{i\nu} \overleftrightarrow{\partial}_{\mu} B_3 + \text{H.c.}, \\ \mathcal{L}_{BB\sigma} &= \ell_S \sigma \sum_{i=0,1} \bar{B}_i^{\mu} B_{j\mu}, \\ \mathcal{L}_{B_3 B_3 \sigma} &= i \ell_{B\sigma} \bar{B}_3 B_3,\end{aligned}\quad (3)$$

where  $B_{i\mu}$  is defined as

$$(B_{0\mu}^{ab}, B_{1\mu}^{ab}) \equiv \left( -\sqrt{\frac{1}{3}}(\gamma_\mu + v_\mu)\gamma^5 B^{ab}, B_\mu^{*ab} \right), \quad (4)$$

and the bottomed baryon matrices are defined as

$$B_{\bar{3}} = \begin{pmatrix} 0 & \Lambda_b^+ & \Xi_b^+ \\ -\Lambda_b^+ & 0 & \Xi_b^0 \\ -\Xi_c^+ & -\Xi_b^0 & 0 \end{pmatrix}, \quad B = \begin{pmatrix} \Sigma_b^{++} & \frac{1}{\sqrt{2}}\Sigma_b^+ & \frac{1}{\sqrt{2}}\Xi_b^{\prime+} \\ \frac{1}{\sqrt{2}}\Sigma_b^+ & \Sigma_b^0 & \frac{1}{\sqrt{2}}\Xi_b^{\prime0} \\ \frac{1}{\sqrt{2}}\Xi_b^{\prime+} & \frac{1}{\sqrt{2}}\Xi_b^{\prime0} & \Omega_b^0 \end{pmatrix}. \quad (5)$$

In the calculation, the masses of particles are chosen as suggested central values in the Review of Particle Physics (PDG) [37]. The mass of broad  $\sigma$  meson is chosen as 500 MeV. The coupling constants involved was cited from the literature [15, 36, 38, 39], and listed in Table 1,

**Table 1** The coupling constants adopted in our calculation. The  $\lambda$  and  $\lambda_{S,I}$  are in the unit of  $\text{GeV}^{-1}$ . Others are in the unit of 1.

$\beta$	$g$	$g_V$	$\lambda$	$g_s$			
0.9	0.59	5.9	0.56	0.76			
$\beta_S$	$\ell_S$	$g_1$	$\lambda_S$	$\beta_B$	$\ell_B$	$g_4$	$\lambda_I$
-1.74	6.2	-0.94	-3.31	$-\beta_S/2$	$-\ell_S/2$	$3g_1/(2\sqrt{2})$	$-\lambda_S/\sqrt{8}$

With the vertices obtained from the above Lagrangians, the potential of couple-channel interaction can be constructed. Because six channels are involved in the current work, it is tedious and fallible to give explicit 36 potential elements and input them into code. Instead, in this work, we input vertices  $\Gamma$  and propagators  $P$  into code directly, and the potential can be obtained as

$$\mathcal{V}_{\mathbb{P},\sigma} = f_I \Gamma_1 \Gamma_2 P_{\mathbb{P},\sigma} f(q^2), \quad \mathcal{V}_{\mathbb{V}} = f_I \Gamma_{1\mu} \Gamma_{2\nu} P_{\mathbb{V}}^{\mu\nu} f(q^2), \quad (6)$$

The propagators are defined as usual as

$$P_{\mathbb{P},\sigma} = \frac{i}{q^2 - m_{\mathbb{P},\sigma}^2}, \quad P_{\mathbb{V}}^{\mu\nu} = i \frac{-g^{\mu\nu} + q^\mu q^\nu / m_{\mathbb{V}}^2}{q^2 - m_{\mathbb{V}}^2}, \quad (7)$$

where the form factor  $f(q^2)$  is adopted to compensate the off-shell effect of exchanged meson as  $f(q^2) = e^{-(m_e^2 - q^2)^2 / \Lambda_e^2}$ , with  $m_e$  being the  $m_{\mathbb{P},\mathbb{V},\sigma}$  and  $q$  being the momentum of the exchanged mesons. The cutoff is rewritten as a form of  $\Lambda_e = m + \alpha_e 0.22 \text{ GeV}$ . The  $f_I$  is the flavor factor for certain meson exchange of certain interaction, and the explicit values are listed in Table 2.

**Table 2** The flavor factors for certain meson exchanges of certain interaction. The values in bracket are for the case of  $I = 3/2$  if the values are different from these of  $I = 1/2$ .

	$\pi$	$\eta$	$\rho$	$\omega$	$\sigma$
$B^{(*)}\Sigma_b^{(*)} \rightarrow B^{(*)}\Sigma_b^{(*)}$	$-1[\frac{1}{2}]$	$\frac{1}{6}[\frac{1}{6}]$	$-1[\frac{1}{2}]$	$\frac{1}{2}[\frac{1}{2}]$	1
$B^{(*)}\Lambda_b \rightarrow B^{(*)}\Lambda_b$	0	0	0	1	2
$B^{(*)}\Lambda_b \rightarrow B^{(*)}\Sigma_b^{(*)}$	$\frac{\sqrt{6}}{2}$	0	$\frac{\sqrt{6}}{2}$	0	0

With the potential kernel obtained, we use the qBSE to solve the scattering amplitude [40–44]. After partial-wave decomposition and spectator quasipotential approximation, the 4-dimensional Bethe-Salpeter equation in the Minkowski space can be reduced to a 1-dimensional equation with fixed spin-parity  $J^P$  as [41],

$$i\mathcal{M}_{\lambda'\lambda}^{J^P}(\mathbf{p}', \mathbf{p}) = i\mathcal{V}_{\lambda'\lambda}^{J^P}(\mathbf{p}', \mathbf{p}) + \sum_{\lambda''} \int \frac{p''^2 dp''}{(2\pi)^3} \cdot i\mathcal{V}_{\lambda'\lambda''}^{J^P}(\mathbf{p}', \mathbf{p}'') G_0(\mathbf{p}'') i\mathcal{M}_{\lambda''\lambda}^{J^P}(\mathbf{p}'', \mathbf{p}), \quad (8)$$

where the sum extends only over nonnegative helicity  $\lambda''$ . Here, the reduced propagator with the spectator approximation can be written as  $G_0(\mathbf{p}'') = \delta^+(p''^2 - m_h^2) / (p_l''^2 - m_l^2)$  with  $p_{h,l}''$  and  $m_{h,l}$  being the momenta and masses of heavy or light constituent particles. The partial wave potential is defined with the potential of interaction obtained in the above in Eq. (6) as

$$\mathcal{V}_{\lambda'\lambda}^{J^P}(\mathbf{p}', \mathbf{p}) = 2\pi \int d\cos\theta [d_{\lambda\lambda'}^J(\theta) \mathcal{V}_{\lambda'\lambda}(\mathbf{p}', \mathbf{p}) + \eta d_{-\lambda\lambda'}^J(\theta) \mathcal{V}_{\lambda'\lambda}(\mathbf{p}', \mathbf{p})], \quad (9)$$

where  $\eta = PP_1 P_2 (-1)^{J-J_1-J_2}$  with  $P$  and  $J$  being parity and spin for system,  $B^{(*)}$  meson or  $\Sigma_b^{(*)}$  baryon. The initial and final relative momenta are chosen as  $\mathbf{p} = (0, 0, p)$  and  $\mathbf{p}' = (p' \sin\theta, 0, p' \cos\theta)$ . The  $d_{\lambda\lambda'}^J(\theta)$  is the Wigner d-matrix. we also adopt an exponential regularization by introducing a form factor into the propagator as [41]

$$G_0(\mathbf{p}'') \rightarrow G_0(\mathbf{p}'') \left[ e^{-(p_l''^2 - m_l^2)^2 / \Lambda_r^4} \right]^2. \quad (10)$$

In the current work, the relation of the cutoff  $\Lambda_r = m + \alpha_r 0.22 \text{ GeV}$  with  $m$  being the mass of the exchanged meson is also introduced into the regularization form factor to suppress large momentum, *i. e.*, the short-range contribution of the  $\pi$  exchange as warned in Ref. [45].

### 3 Numerical results

The 1-dimensional integral equation can be transformed into a matrix equation as  $M = V + VG_0M$  by Gauss discretization. The molecular states can be found by searching for the pole of scattering amplitude  $M$  in complex energy plane at  $|1 - V(z)G(z)| = 0$  with  $z = W + iI/2$  equaling to system energy  $W$  at real axis [41]. In addition, we take two free parameters  $\alpha_e$  and  $\alpha_r$  as  $\alpha$  for simplification.

#### 3.1 Single-channel results

Each experimental observed  $P_c$  state is close to a threshold, respectively [2, 3]. It suggests that each of these states should be mainly from a single-channel interaction in the

molecular state picture, which is confirmed by previous study in Ref. [24]. In this work, we present the single-channel results first.

In the current work, we consider all states with spin parities which can be produced from S-wave interaction,  $\Sigma_b^* B^*$  with  $1/2^-, 3/2^-, 5/2^-$ ,  $\Sigma_b B^*$  with  $1/2^-, 3/2^-$ ,  $\Sigma_b^* B$  with  $3/2^-$  and  $\Sigma_b B$  with  $1/2^-$ . The results for isodoublet with  $I = 1/2$  are illustrated in Fig. 1. The  $\Lambda_b B^{(*)}$  with  $1/2^-, 3/2^-$  and  $\Lambda_b B$  with  $1/2^-$  are also calculated, however, large  $\alpha$  beyond reasonable limit is required to produce bound states.

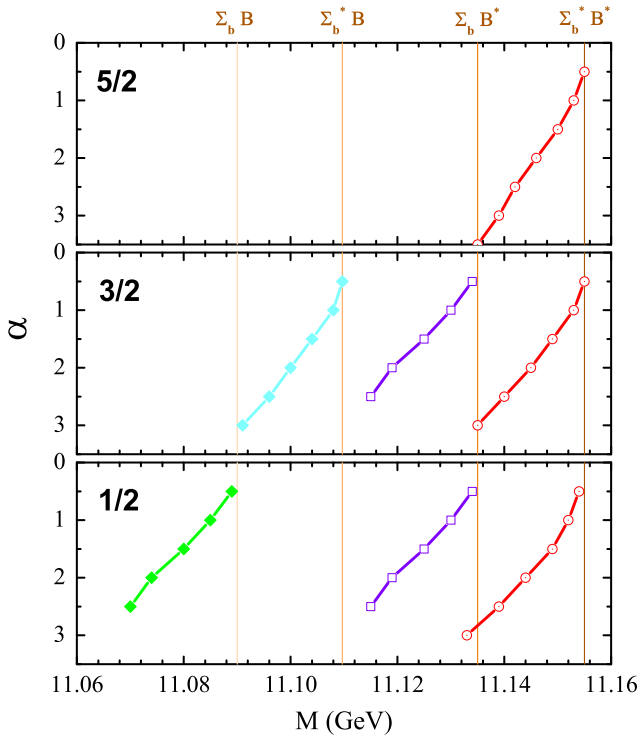


**Fig. 1** The  $\alpha$  dependence of the mass  $M$  of isodoublet binding states from single-channel interaction. The four solid lines from right to left represent the thresholds of four channels  $\Sigma_b^* B^*$ ,  $\Sigma_b B^*$ ,  $\Sigma_b^* B$  and  $\Sigma_b B$  at 11155MeV, 11135MeV, 11110MeV and 11090MeV, respectively. The curves are for the bound states from the interactions with corresponding thresholds.

The results suggest that bound states can be produced in all seven cases in a range of  $\alpha$  from 0 to 3.5. All states appear at  $\alpha$  about 0.5, and binding becomes deeper with the increase of  $\alpha$ , and gradually reach to a binding energy about 20 MeV or the next threshold at  $\alpha = 2.5 - 3.5$ . The binding energies will continue to increase, but we no longer present such results. The trends of curves for three states produced from the  $\Sigma_b^* B^*$  interaction with different spin parities are almost the same. Such phenomenon can also be found for two curves for two states from the  $\Sigma_b B^*$  interaction. Compared with the results for  $P_c$  states [23, 24], one can find that the values of parameter  $\alpha$  to produce the hidden-bottom molecular states is relatively smaller.

In Fig 2, we present the results for isoquartet states with  $I = 3/2$ . In the calculation, we also consider seven cases as

for isodoublet. No bound state is produced from  $\Sigma_b B$  interaction with  $(1/2^-)$  and  $\Sigma_b^* B$  interaction from  $(3/2^-)$  even if  $\alpha$  is taken to 9. Except these two states, left five states can be produced from single-channel interaction as shown in 2, but with considerably large  $\alpha$ . The production of bound states,  $\Sigma_b^* B^*(1/2^-)$ ,  $\Sigma_b B^*(1/2^-)$  and  $\Sigma_b^* B^*(3/2^-)$ , needs a value of  $\alpha$  at least 4, which is larger than the maximum value of  $\alpha$  required for binding of isodoublet molecular states with  $I = 1/2$ . It indicates that these three states are hardly to be found if the isodoublet states have small binding energies. The rest two states  $\Sigma_b B^*(3/2^-)$  and  $\Sigma_b^* B^*(5/2^-)$  appears at  $\alpha = 3$  and 2.5, respectively. It implies that these two molecular states may exist if the isodoublet states are deeply bound. Generally speaking, if we assume that the  $P_b$  states are also loosely bound states as  $P_c$  states, the possibility of existence of isoquartet states is very small. In Ref [25], within the frame of constituent quark model, the molecular states with  $I = 3/2$  were also not found.

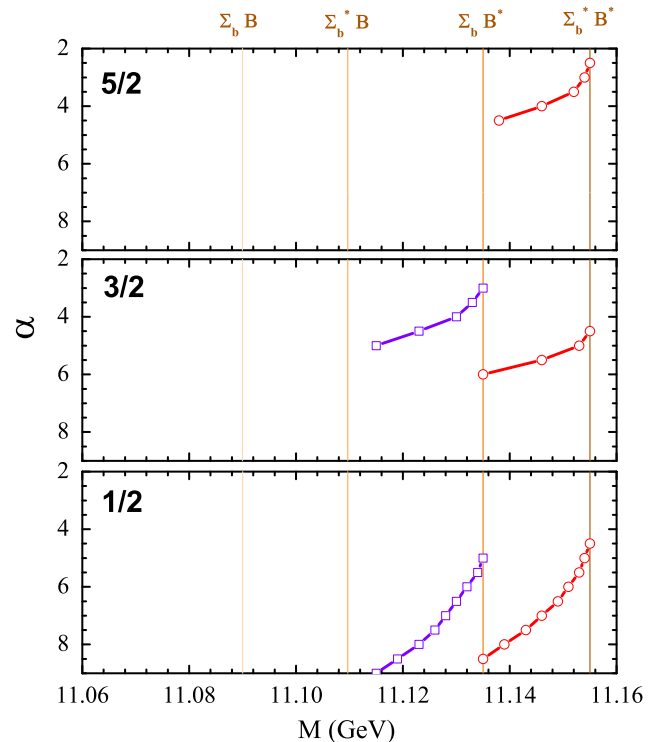


**Fig. 2** The mass  $M$  with the variation of the  $\alpha$  for isoquartet bound states. Other conventions are the same as in Fig. 1.

### 3.2 Coupled-channel results

In the previous calculation, the bound states from single channel calculation exhibit as poles at real axis of complex energy plane, that is, the widths of these states are zero. In the case of the  $P_c$  states, we found that the experimental width can be well reproduced with inclusion of coupled-channel effect [24]. In the above single-channel calculation, seven bound states are produced. Those states can be coupled to each other by exchanges of light mesons. Besides,

the  $\Lambda\bar{D}^*$  channel is also found important for the width of  $P_c$  states [24, 29, 30]. In the following, coupled-channel results for the  $\Sigma_b^{(*)}B^{(*)} - \Lambda_b B^{(*)}$  interaction will be given.

Here, we first give an example to show a general picture of coupled-channel results. Since there is no experimental data about the  $P_b$  states, we should choose a parameter to present the results. The only free parameter in our model is  $\alpha$ , and in the single-channel calculation the  $\alpha$  dependences of the masses of seven bound states exhibit a similar trend. Hence, we choose  $\alpha$  as 1.5 to illustrate the poles from coupled-channel  $\Sigma_b^{(*)}B^{(*)} - \Lambda_b B^{(*)}$  interaction in Fig. 3. The values of  $\log|1 - V(z)G_0(z)|$  with variation of complex energy  $z$  is adopted to show the positions of poles of coupled-channel scattering amplitude because  $M = (1 - VG_0)^{-1}V$ . And we present the results for spin parities  $5/2^-$ ,  $3/2^-$ , and  $1/2^-$  in a range from 11.06 to 11.16 GeV for real part of complex energy  $Re(z)$  and -2 to 2 MeV for imaginary part  $Im(z)$ .

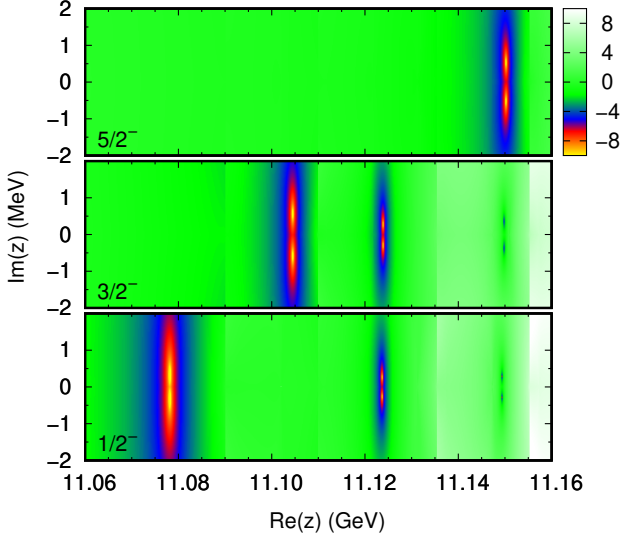


**Fig. 3** The  $\log|1 - V(z)G_0(z)|$  with the variation of  $z$  for coupled-channel  $\Sigma_b^{(*)}B^{(*)} - \Lambda_b B^{(*)}$  interaction with  $J^P = 1/2^-, 3/2^-$  and  $5/2^-$  at  $\alpha = 1.5$ . The color means the value of  $\log|1 - V(z)G_0(z)|$  as shown in the color box.

One can find that there are still seven poles produced as in the single-channel calculation. It suggests that only states with an S-wave interaction can be produced for three spin parities considered. In the case with  $J^P = 1/2^-$ , there exist three poles near the  $\Sigma_b B$  (S wave),  $\Sigma_b B^*$  (S and D waves) and  $\Sigma_b^* B^*$  (S, D and G waves) thresholds, respectively. No pole appears near  $\Sigma^* B$  (P wave) threshold for  $1/2^-$ . In the case with  $J^P = 3/2^-$ , we also have three poles near the  $\Sigma_b B$  (S and D waves),  $\Sigma_b B^*$  (S and D waves) and  $\Sigma_b^* B^*$  (S, D and G waves) thresholds, respectively. And no pole appears near  $\Sigma_b B$  (P wave) threshold. For spin parity  $5/2^-$  there is only one pole near the  $\Sigma_b^* B^*$  thresholds, and only this channel can produce a pole with  $5/2^-$  in S wave.

The  $P_c(4457)$  and  $P_c(4440)$  is close to each other near  $\Sigma_c \bar{D}^*$  threshold, which was even taken as one resonance structure in the first observation of the  $P_c$  states [2]. In the  $P_b$  case, our results exhibit a more serious overlapping between two states near  $\Sigma_b B^*$  as in the single channel calculation. As shown in Fig. 3, these two poles with  $1/2^-$  and  $3/2^-$  have almost the same mass and width. Furthermore, the masses of three poles near the  $\Sigma_b^* B^*$  threshold are also close very much, which are 11149.2 MeV, 11149.7 MeV and 11150.1 MeV corresponding to the two molecular states with  $1/2^-$ ,  $3/2^-$  and  $5/2^-$ , respectively. Different from the  $P_c$  states [24], here, the state with  $5/2^-$  stands out background obviously while other two poles with  $J^P = 1/2^-$  and  $3/2^-$  are very dimly, and may be difficult to be found at experiment.

As shown in the figure, the poles acquire imaginary parts after coupled-channel effects are included in the calculation. However, these states are generally very narrow, with imaginary parts smaller than 0.5 MeV. By using the relation  $\Gamma = -2 \text{Im}(z)$ , it means a small width about 1 MeV or smaller, which is much smaller than the  $P_c$  states with similar binding energy. It is worth mentioning that at  $\alpha = 1.5$ , except for  $\Sigma_b^* B^*(5/2^-)$ , the masses of six molecular states after inclusion of coupled-channel effect are in good agreement with the results obtained under the frame of the constituent quark model in Ref [17].

In the above, we only present the poles of molecular states obtained by the coupled-channels calculation at a value of  $\alpha = 1.5$ . Because there is no experimental data, in the following, we will present the results with different values of  $\alpha$  from 0.5 to 2.0 to show the dependence of results on the parameter in second and third columns of Table 3. The two-channel calculation results are also listed in the fourth to eighth columns to show the role of each channel on widths of molecular states. Here, to emphasize the nearest threshold, we replace the real part of pole by  $z \rightarrow M_{th} - z$  with  $M_{th}$  being the mass of nearest higher threshold.

In the first column, we list thresholds with certain spin parity, and the result of pole under the corresponding threshold with different  $\alpha$  is given in the second and third columns with full coupled-channel  $\Sigma_b^{(*)}B^{(*)} - \Lambda_b B^{(*)}$  interaction. One can find, except a small width is acquired, the results are similar to those from the single-channel calculation. Hence, we take such channel as production channel of this pole. All poles appear on threshold at about  $\alpha = 0.5$  and leave the threshold with the increasing of  $\alpha$ . If we chosen a binding energy about 10 MeV, the widths of most states are very small, about 1 MeV or smaller.

In the fourth to eighth columns, we consider two-channel result with the coupling between the production channel and a channel below it. The imaginary part reflects the strength of couplings between two channels. Since the pole is mainly from the production channel, the effect a

**Table 3** The masses and widths of molecular states at different values of  $\alpha$ . The “CC” means full coupled-channel calculation. The values of the complex position means mass of corresponding threshold subtracted by the position of a pole,  $M_{th} - z$ , in the unit of MeV. The two short line “--” means the coupling does not exist. The imaginary part of some poles are shown as “0.00”, which means too small value under the current precision chosen.

	$\alpha_r$	CC	$\Sigma_b B^*$	$\Sigma_b^* B$	$\Sigma_b B$	$\Lambda_b B^*$	$\Lambda_b B$
$\Sigma_b^* B^*(1/2^-)$ $M_{th} = 11155\text{MeV}$	0.6	0.6+0.02i	0.6+0.01i	0.6+0.01i	0.6+0.01i	0.6+0.00i	0.6+0.00i
	1.0	2.4+0.09i	2.5+0.03i	2.5+0.03i	2.5+0.04i	2.5+0.02i	2.5+0.00i
	1.5	5.8+0.28i	6.1+0.07i	6.0+0.10i	6.0+0.16i	6.0+0.16i	6.1+0.00i
	2.0	9.6+0.40i	10.3+0.24i	10.4+0.25i	9.9+0.31i	10.3+0.63i	10.5+0.00i
$\Sigma_b^* B^*(3/2^-)$ $M_{th} = 11155\text{MeV}$	0.6	0.5+0.03i	0.5+0.02i	0.5+0.01i	0.5+0.00i	0.5+0.00i	0.5+0.00i
	1.0	2.2+0.10i	2.3+0.04i	2.3+0.03i	2.3+0.02i	2.3+0.01i	2.3+0.00i
	1.5	5.3+0.36i	5.5+0.07i	5.7+0.03i	5.6+0.08i	5.6+0.12i	5.6+0.03i
	2.0	8.6+1.38i	9.3+0.19i	9.8+0.09i	9.8+0.16i	9.4+0.48i	9.7+0.17i
$\Sigma_b^* B^*(5/2^-)$ $M_{th} = 11155\text{MeV}$	0.6	0.4+0.04i	0.4+0.01i	0.4+0.01i	0.4+0.01i	0.4+0.00i	0.4+0.00i
	1.0	2.1+0.15i	2.4+0.01i	2.1+0.05i	2.0+0.01i	2.1+0.01i	2.1+0.00i
	1.5	4.9+0.52i	5.3+0.01i	5.1+0.02i	5.0+0.27i	4.9+0.25i	5.0+0.07i
	2.0	8.6+1.38i	9.3+0.19i	9.8+0.09i	9.8+0.16i	9.4+0.48i	9.7+0.17i
$\Sigma_b B^*(1/2^-)$ $M_{th} = 11135\text{MeV}$	0.5	1.4+0.01i	--	1.2+0.00i	1.2+0.00i	1.2+0.00i	1.2+0.00i
	1.0	5.7+0.05i	--	5.0+0.01i	5.0+0.02i	5.0+0.01i	5.0+0.00i
	1.5	11.4+0.26i	--	10.0+0.05i	10.1+0.05i	10.0+0.07i	10.1+0.03i
	2.0	17.6+0.70i	--	15.7+0.25i	16.1+0.09i	15.7+0.22i	15.9+0.03i
$\Sigma_b B^*(3/2^-)$ $M_{th} = 11135\text{MeV}$	0.5	1.4+0.02i	--	1.2+0.00i	1.2+0.00i	1.2+0.00i	1.2+0.00i
	1.0	5.7+0.17i	--	5.1+0.01i	5.1+0.14i	5.1+0.02i	5.1+0.00i
	1.5	11.2+0.28i	--	10.1+0.02i	10.3+0.22i	10.0+0.20i	10.1+0.05i
	2.0	17.2+0.45i	--	15.7+0.03i	16.2+0.33i	15.0+0.81i	15.5+0.31i
$\Sigma_b^* B(3/2^-)$ $M_{th} = 11110\text{MeV}$	1.0	2.4+0.08i	--	--	2.4+0.00i	2.4+0.07i	2.4+0.00i
	1.5	5.5+0.57i	--	--	5.7+0.00i	5.4+0.49i	5.7+0.00i
	2.0	8.4+2.05i	--	--	9.6+0.00i	8.8+1.56i	9.6+0.00i
$\Sigma_b B(1/2^-)$ $M_{th} = 11090\text{MeV}$	0.5	1.6+0.00i	--	--	--	1.4+0.00i	1.4+0.00i
	1.0	6.0+0.04i	--	--	--	5.3+0.04i	5.3+0.00i
	1.5	11.8+0.33i	--	--	--	10.2+0.25i	10.4+0.00i
	2.0	17.9+1.60i	--	--	--	15.4+1.17i	16.1+0.00i

channel on the pole can be also estimated from the two-channel results. Because the width with smaller  $\alpha$  is very small, in the followings, we focus on the results at larger  $\alpha$ , 1.5 and 2.0.

Three states near  $\Sigma_b^* B^*$  threshold, which is the highest threshold of channels considered in the current work, can decay into five channels. Among these decay channels, the  $\Lambda_b B^*$  channel has strongest couplings to this three states. For the two states near  $\Sigma_b B^*$  threshold, there are four decay channels, the  $\Lambda_b B^*$  channel is much stronger than other channels for  $3/2^-$ . For  $1/2^-$  state, both  $\Sigma_b^* B$  and  $\Lambda_b B^*$  channels couples strongly to the  $\Sigma_b B^*$  channel. Among three possible decay channels of the state near  $\Sigma_b^* B$  thresholds,

only  $\Lambda_b B^*$  channel provides large width, and other channels only give very small imaginary part of the position. For the  $\Sigma_b B(1/2^-)$  case, only  $\Lambda_b B^{(*)}$  channels involves, among which, the  $\Lambda_b B^*$  channel is still dominant one. Hence, for all seven states, the  $\Lambda_b B^*$  channel is the most important one in all channels considered, which is consistent with the results of the hidden-charm pentaquarks in Refs. [24, 29, 30].

#### 4 Summary and discussion

In this work, the masses and widths of hidden-bottom molecular pentaquarks are predicted from coupled-channel

$\Sigma_b^{(*)}B^{(*)} - \Lambda_b B^{(*)}$  interaction in the qBSE approach with the help of effective Lagrangians with heavy quark and chiral symmetries. The results suggest that seven molecular states can be produced from the interactions.

Among the seven states, three of them are near the  $\Sigma_b^{(*)}B^{(*)}$  threshold, and the masses of these three states are very close. The two states with  $1/2^-$  and  $3/2^-$  are very weak compared with the state with  $5/2^-$ . Hence, these three states should exhibit as one resonance structure without partial wave analysis. Even with partial wave analysis, the states with  $1/2^-$  and  $3/2^-$  are difficult to be distinguished from the one with  $5/2^-$ . The two states near  $\Sigma_b B^*$  are also mixing together but a partial-wave analysis will be helpful to distinguish them. Hence, the results suggest that four resonance structures may be observed in experiment, though there exist seven molecular states from coupled-channel  $\Sigma_b^{(*)}B^{(*)} - \Lambda_b B^{(*)}$  interaction.

Compared with hidden-charm  $P_c$  states, the widths of  $P_b$  states are much smaller, about 1 MeV or smaller. And the calculation suggests that the  $\Lambda_b D^*$  channel has strong couplings to the molecular states. The small width have both advantage and disadvantage in experimental observation of such states. The small width makes the production possibility small, which needs high luminosity of experimental facility. However, a small width also makes the peak of state stand out obviously from background in experiment. In Ref. [31], we study the possibility to search for such states in pion and photon induced productions. The results suggest that with small widths the measurement of the  $P_b$  states is promising at the such as the COMPASS J-PARC, especially the Electron Ion Collider (EicC) in China.

**Acknowledgement** This project is supported by the National Natural Science Foundation of China with Grants No. 11675228.

## References

- H. X. Chen, W. Chen, X. Liu and S. L. Zhu, “The hidden-charm pentaquark and tetraquark states,” Phys. Rept. **639** (2016), 1-121 [arXiv:1601.02092 [hep-ph]].
- R. Aaij *et al.* [LHCb Collaboration], “Observation of a narrow pentaquark state,  $P_c(4312)^+$ , and of two-peak structure of the  $P_c(4450)^+$ ,” Phys. Rev. Lett. **122** (2019) no.22, 222001 [arXiv:1904.03947 [hep-ex]].
- R. Aaij *et al.* [LHCb Collaboration], “Observation of  $J/\psi p$  Resonances Consistent with Pentaquark States in  $\Lambda_b^0 \rightarrow J/\psi K^- p$  Decays,” Phys. Rev. Lett. **115** (2015) 072001 [arXiv:1507.03414 [hep-ex]].
- J. J. Wu, R. Molina, E. Oset and B. S. Zou, “Prediction of narrow  $N^*$  and  $\Lambda^*$  resonances with hidden charm above 4 GeV,” Phys. Rev. Lett. **105**, 232001 (2010).
- W. L. Wang, F. Huang, Z. Y. Zhang and B. S. Zou, “ $\Sigma_c \bar{D}$  and  $\Lambda_c \bar{D}$  states in a chiral quark model,” Phys. Rev. C **84** (2011) 015203 [arXiv:1101.0453 [nucl-th]].
- Z. C. Yang, Z. F. Sun, J. He, X. Liu and S. L. Zhu, “The possible hidden-charm molecular baryons composed of anti-charmed meson and charmed baryon,” Chin. Phys. C **36**, 6 (2012) [arXiv:1105.2901 [hep-ph]].
- J. J. Wu, T.-S. H. Lee and B. S. Zou, “Nucleon Resonances with Hidden Charm in Coupled-Channel Models,” Phys. Rev. C **85** (2012) 044002 [arXiv:1202.1036 [nucl-th]].
- S. G. Yuan, K. W. Wei, J. He, H. S. Xu and B. S. Zou, “Study of  $qqqc\bar{c}$  five quark system with three kinds of quark-quark hyperfine interaction,” Eur. Phys. J. A **48** (2012), 61 [arXiv:1201.0807 [nucl-th]].
- R. Chen, X. Liu, X. Q. Li and S. L. Zhu, “Identifying exotic hidden-charm pentaquarks,” Phys. Rev. Lett. **115**, no. 13, 132002 (2015) [arXiv:1507.03704 [hep-ph]].
- H. X. Chen, W. Chen, X. Liu, T. G. Steele and S. L. Zhu, “Towards exotic hidden-charm pentaquarks in QCD,” Phys. Rev. Lett. **115**, no. 17, 172001 (2015) [arXiv:1507.03717 [hep-ph]].
- M. Karliner and J. L. Rosner, “New Exotic Meson and Baryon Resonances from Doubly-Heavy Hadronic Molecules,” Phys. Rev. Lett. **115** (2015) no.12, 122001 [arXiv:1506.06386 [hep-ph]].
- L. Roca, J. Nieves and E. Oset, “LHCb pentaquark as a  $\bar{D}^* \Sigma_c - \bar{D}^* \Sigma_c^*$  molecular state,” Phys. Rev. D **92**, no. 9, 094003 (2015) [arXiv:1507.04249 [hep-ph]].
- J. He, “ $\bar{D} \Sigma_c^*$  and  $\bar{D}^* \Sigma_c$  interactions and the LHCb hidden-charmed pentaquarks,” Phys. Lett. B **753**, 547 (2016) [arXiv:1507.05200 [hep-ph]].
- J. He, “Understanding spin parity of  $P_c(4450)$  and  $Y(4274)$  in a hadronic molecular state picture,” Phys. Rev. D **95**, no. 7, 074004 (2017) [arXiv:1607.03223 [hep-ph]].
- R. Chen, X. Liu, Z. F. Sun and S. L. Zhu, “Strong LHCb evidence for supporting the existence of hidden-charm molecular pentaquarks,” arXiv:1903.11013 [hep-ph].
- C. Fernandez-RamiÅnrez *et al.* [JPAC Collaboration], “Interpretation of the LHCb  $P_c(4312)$  Signal,” Phys. Rev. Lett. **123** (2019) no.9, 092001 [arXiv:1904.10021 [hep-ph]].
- H. Huang and J. Ping, “Investigating the hidden-charm and hidden-bottom pentaquark resonances in scattering process,” Phys. Rev. D **99** (2019) no.1, 014010 [arXiv:1811.04260 [hep-ph]].
- T. J. Burns, “Phenomenology of  $P_c(4380)^+$ ,  $P_c(4450)^+$  and related states,” Eur. Phys. J. A **51** (2015) no.11, 152 [arXiv:1509.02460 [hep-ph]].
- U. G. Meißner and J. A. Oller, “Testing the  $\chi_{c1} p$  composite nature of the  $P_c(4450)$ ,” Phys. Lett. B **751** (2015), 59-62 [arXiv:1507.07478 [hep-ph]].

20. R. F. Lebed, “The Pentaquark Candidates in the Dynamical Diquark Picture,” *Phys. Lett. B* **749** (2015), 454-457 [arXiv:1507.05867 [hep-ph]].
21. H. X. Chen, W. Chen and S. L. Zhu, “Possible interpretations of the  $P_c(4312)$ ,  $P_c(4440)$ , and  $P_c(4457)$ ,” arXiv:1903.11001 [hep-ph].
22. M. Z. Liu, Y. W. Pan, F. Z. Peng, M. Sanchez Sanchez, L. S. Geng, A. Hosaka and M. Pavon Valderrama, “Emergence of a complete heavy-quark spin symmetry multiplet: seven molecular pentaquarks in light of the latest LHCb analysis,” *Phys. Rev. Lett.* **122** (2019) no.24, 242001 [arXiv:1903.11560 [hep-ph]].
23. J. He, “Study of  $P_c(4457)$ ,  $P_c(4440)$ , and  $P_c(4312)$  in a quasipotential Bethe-Salpeter equation approach,” *Eur. Phys. J. C* **79**, no. 5, 393 (2019) [arXiv:1903.11872 [hep-ph]].
24. J. He and D. Y. Chen, “Molecular states from  $\Sigma_c^{(*)}\bar{D}^{(*)} - \Lambda_c\bar{D}^{(*)}$  interaction,” *Eur. Phys. J. C* **79** (2019) no.11, 887 [arXiv:1909.05681 [hep-ph]].
25. G. Yang, J. Ping and J. Segovia, “Hidden-bottom pentaquarks,” *Phys. Rev. D* **99** (2019) no.1, 014035 [arXiv:1809.06193 [hep-ph]].
26. B. Wang, L. Meng and S. L. Zhu, “Hidden-charm and hidden-bottom molecular pentaquarks in chiral effective field theory,” *JHEP* **11** (2019), 108 [arXiv:1909.13054 [hep-ph]].
27. H. W. Ke, M. Li, X. H. Liu and X. Q. Li, “Study on possible molecular states composed of  $\Lambda_c\bar{D}$  ( $\Lambda_b B$ ) and  $\Sigma_c\bar{D}$  ( $\Sigma_b B$ ) within the Bethe-Salpeter framework,” *Phys. Rev. D* **101** (2020) no.1, 014024 [arXiv:1909.12509 [hep-ph]].
28. T. Gutsche and V. E. Lyubovitskij, “Structure and decays of hidden heavy pentaquarks,” *Phys. Rev. D* **100** (2019) no.9, 094031 [arXiv:1910.03984 [hep-ph]].
29. Y. H. Lin, C. W. Shen and B. S. Zou, “Decay behavior of the strange and beauty partners of  $P_c$  hadronic molecules,” *Nucl. Phys. A* **980** (2018) 21 [arXiv:1805.06843 [hep-ph]].
30. Y. H. Lin and B. S. Zou, “Strong decays of the latest LHCb pentaquark candidates in hadronic molecule pictures,” *Phys. Rev. D* **100** (2019) no.5, 056005 [arXiv:1908.05309 [hep-ph]].
31. X. Y. Wang, J. He and X. Chen, “Systematic study of the production of hidden-bottom pentaquarks via  $\gamma p$  and  $\pi^- p$  scatterings,” *Phys. Rev. D* **101** (2020) no.3, 034032 [arXiv:1912.07156 [hep-ph]].
32. H. Y. Cheng, C. Y. Cheung, G. L. Lin, Y. C. Lin, T. M. Yan and H. L. Yu, “Chiral Lagrangians for radiative decays of heavy hadrons,” *Phys. Rev. D* **47**, 1030 (1993) [hep-ph/9209262].
33. T. M. Yan, H. Y. Cheng, C. Y. Cheung, G. L. Lin, Y. C. Lin and H. L. Yu, “Heavy quark symmetry and chiral dynamics,” *Phys. Rev. D* **46**, 1148 (1992) Erratum: [*Phys. Rev. D* **55**, 5851 (1997)].
34. M. B. Wise, “Chiral perturbation theory for hadrons containing a heavy quark,” *Phys. Rev. D* **45**, 2188 (1992).
35. R. Casalbuoni, A. Deandrea, N. Di Bartolomeo, R. Gatto, F. Feruglio and G. Nardulli, “Phenomenology of heavy meson chiral Lagrangians,” *Phys. Rept.* **281**, 145 (1997) [hep-ph/9605342].
36. Y. R. Liu and M. Oka, “ $\Lambda_c N$  bound states revisited,” *Phys. Rev. D* **85** (2012) 014015 [arXiv:1103.4624 [hep-ph]].
37. M. Tanabashi *et al.* [Particle Data Group], “Review of Particle Physics,” *Phys. Rev. D* **98**, no. 3, 030001 (2018).
38. C. Isola, M. Ladisa, G. Nardulli and P. Santorelli, “Charming penguins in  $B \rightarrow K^* \pi, K(\rho, \omega, \phi)$  decays,” *Phys. Rev. D* **68**, 114001 (2003) [hep-ph/0307367].
39. A. F. Falk and M. E. Luke, “Strong decays of excited heavy mesons in chiral perturbation theory,” *Phys. Lett. B* **292** (1992) 119 [hep-ph/9206241].
40. J. He, “Study of the  $B\bar{B}^*/D\bar{D}^*$  bound states in a Bethe-Salpeter approach,” *Phys. Rev. D* **90**, no. 7, 076008 (2014) [arXiv:1409.8506 [hep-ph]].
41. J. He, “The  $Z_c(3900)$  as a resonance from the  $D\bar{D}^*$  interaction,” *Phys. Rev. D* **92** (2015) no.3, 034004 [arXiv:1505.05379 [hep-ph]].
42. J. He, D. Y. Chen and X. Liu, “New Structure Around 3250 MeV in the Baryonic B Decay and the  $D_0^*(2400)N$  Molecular Hadron,” *Eur. Phys. J. C* **72** (2012) 2121 [arXiv:1204.6390 [hep-ph]].
43. J. He, “Internal structures of the nucleon resonances  $N(1875)$  and  $N(2120)$ ,” *Phys. Rev. C* **91** (2015) no.1, 018201 [arXiv:1501.00522 [nucl-th]].
44. J. He, “Nucleon resonances  $N(1875)$  and  $N(2100)$  as strange partners of LHCb pentaquarks,” *Phys. Rev. D* **95** (2017) no.7, 074031 [arXiv:1701.03738 [hep-ph]].
45. M. Z. Liu, T. W. Wu, M. Sanchez Sanchez, M. P. Valderrama, L. S. Geng and J. J. Xie, “Spin-parities of the  $P_c(4440)$  and  $P_c(4457)$  in the One-Boson-Exchange Model,” [arXiv:1907.06093 [hep-ph]].